2

CONF-810605--1

# BIAS IDENTIFICATION IN PWR PRESSURIZER INSTRUMENTATION USING THE GENERALIZED LIKELIHOOD-RATIO TECHNIQUE

J. Louis Tylee
EG&G Idaho, Inc.
P.O. Box 1625
Idaho Falls, Idaho 83415





## ABSTRACT

A method for detecting and identifying biases in the pressure and level sensors of a pressurized water reactor (PWR) pressurizer is described. The generalized likelihood ratio (GLR) technique performs statistical tests on the innovations sequence of a Kalman filter state estimator and is capable of determining when a bias appears, in what sensor the bias exists, and estimating the bias magnitude. Simulation results using a second-order linear, discrete PWR pressurizer model demonstrate the capabilities of the GLR method.

Prepared for presentation at the 1981 Joint Automatic Control Conference, Charlottesville, Virginia, June 17-19, 1981.

# BIAS IDENTIFICATION IN PWR PRESSURIZER INSTRUMENTATION USING THE GENERALIZED LIKELIHOOD-RATIO TECHNIQUE

## 1. INTRODUCTION

In a nuclear power plant, failures will occur and must be detected and compensated for before a significant decrease in plant performance results. Figure 1 schematically depicts a power plant. Here, a finite set of sensors provides plant measurements to both an automatic controller and an operator. The controller uses these measurements to compute actuator settings which will provide a set of control inputs to the plant. The operator also acts as a controller in that he uses his knowledge of the plant operation, combined with the plant measurements, to determine if any additional control is needed. If the plant measurements do not coincide with the operator's idea of what those measurements should be, it must be assumed that a system failure has occurred. The operator then has the difficult task of deciding whether the bad measurements are due to a failed sensor, a broken actuator, or due to an unexpected change in the plant process dynamics. During the time needed to identify the failure, plant performance may seriously degrade. Such degradation could perhaps be avoided if some type of system failure monitor could be implemented.

A power plant, augmented with a failure monitor, is shown in Figure 2. Such a failure monitor would most likely consist of an on-line digital computer due to the relatively low cost and programming flexibility. Inputs to the failure monitor include the available plant measurements, the controls calculated by the automatic controller, and the operator controls. Based

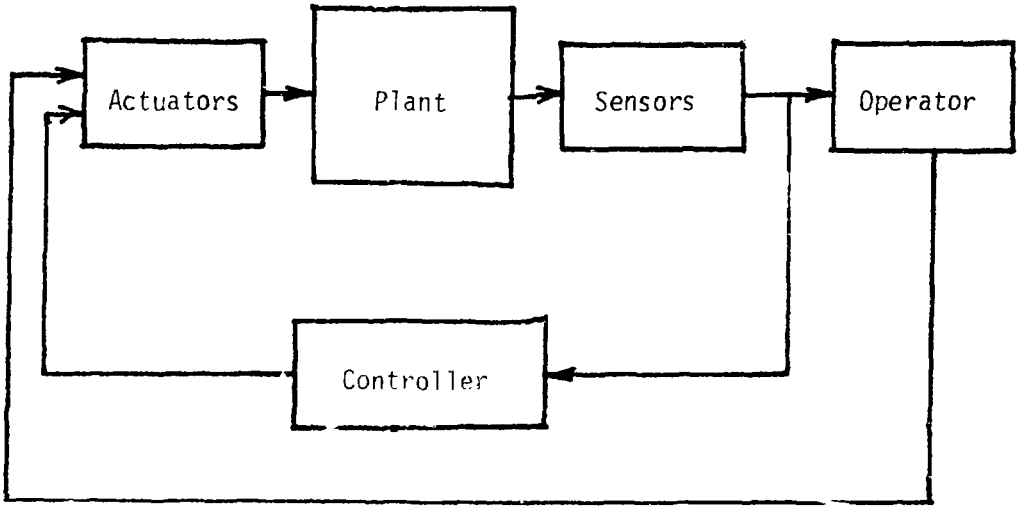


Figure 1. Power Plant Schematic

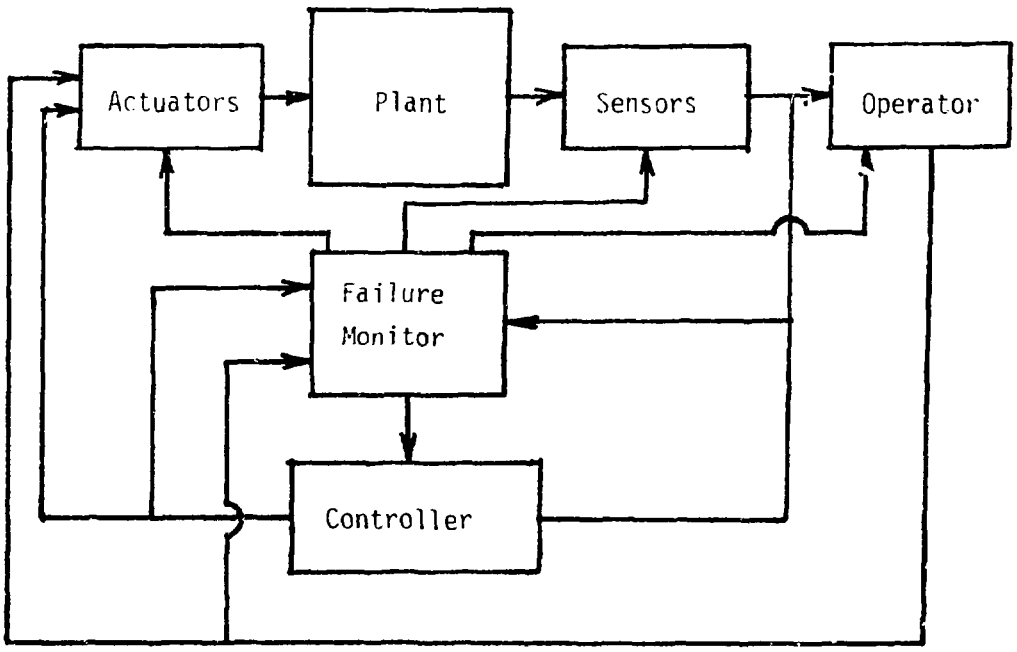


Figure 2. Power Plant Augmented with Failure Monitor

on these inputs, the failure monitor should be able to perform several tasks. Its primary purpose is to continually check the system performance and determine whether it is operating normally. If an abnormality is detected, the monitor should identify and determine the extent of the abnormality and inform the operator of the problem. Finally, the monitor should be able to adjust or reorganize the plant actuators, sensors, and/or controller to avoid severe performance changes. (Although the problem of system reorganization following a failure detection is important, in this paper we will be concerned only with the detection and identification of a system failure.)

Several failure detection schemes for failure monitors similar to the one in Figure 2 have been researched in the past few years [1]. Ideas from simple voting systems to elaborate multiple hypothesis probabilistic techniques have been studied and many successful applications reported. An extremely powerful class of detection schemes are those that perform statistical tests on the innovations sequence of a Kalman filter designed for the operating dynamic system. A Kalman filter is simply a set of mathematical algorithms that generate optimal estimates of the plant measurements using knowledge of the system dynamics. The filter innovations is then the difference between the actual plant measurements and the Kalman filter estimates. One of the more successful statistical tests on the innovations used to identify failures, and the one described here, is known as the generalized likelihood ratio (GLR) method [2]. Briefly, the GLR method employs mathematical descriptions of various failure modes to perform multiple hypothesis testing and ascertain if a failure has occurred. Furthermore, if a failure is detected, the GLR method determines when the failure occurred, what kind of failure it is, and estimates the magnitude of the failure. This information would be invaluable to the plant operator trying to compensate for a failure.

In this paper, a GLR failure monitor for a pressurized water reactor (PWR) pressurizer is developed. The monitor is restricted to only identifying biases in the pressurizer instrumentation. This restriction was made to demonstrate the applicability of the GLR methods to nuclear components with a minimum of computational complexity. Future modifications to the failure monitor include the ability to detect changes in pressurizer dynamics, failures in pressurizer control actuators, and complete failures of sensors. We first describe the GLR equations, including the required plant dynamics and Kalman filter formulations. Next, a second-order model of the pressurizer dynamics for use in the failure monitor is developed. Finally, the ability of the GLR method to identify biases is investigated using simulated plant transient data.

## 2. GLR FAILURE MONITOR EQUATIONS

The GLR method employs two steps in the identification of failures. The first involves using a Kalman filter, designed for the unfailed system, to generate the innovations, or residuals sequence. In the second step, using descriptions of various hypothesized failure modes (e.g., in this paper, sensor biases) and the innovations, the log-likelihood ratio, is computed and maximized. Comparing this maximum ratio to a predetermined threshold value yields the failure decision.

Both the Kalman filter and log-likelihood ratio calculations require a description of the plant dynamics. In this section, we present the required form of the plant state and measurement equations, the filter equations, and the log-likelihood ratio computational procedure.

### 2.1 Plant Dynamics Equations

In this work, we assume the plant dynamics can be modeled as a linear, time-varying, discrete system of the form:

$$x(k+1)=\Phi(k+1,k)x(k) + \Theta(k)u(k) + w(k) \quad (1)$$

where $x(k)$ is the plant state vector at time k, $u(k)$ a deterministic control input, and $w(k)$ a zero-mean, white disturbance vector. Also, $\Phi(k+1,k)$ is the state transition matrix from k to k+1, and $\Theta(k)$ is the control matrix.

Similarly, a model of the plant measurements is required. This must be a linear model of the form:

$$y(k) = C(k)x(k) + v(k) \quad (2)$$

where $v(k)$ is a zero-mean, white measurement noise, uncorrelated with the process noise $w(k)$, and $C(k)$ is the required measurement system matrix. Plant model statistics required by the Kalman filter include the covariance of the two white noise processes $w(k)$ and $v(k)$, an initial estimate of the state vector $x(0)$ and the variance in the estimate of $x(0)$.

## 2.2 Kalman Filter Equations

The mathematics of the Kalman filter have been derived in several texts [3] and no attempt is made to reproduce such derivations here. Instead, the equations are presented with a brief description of what each one does.

At time k a plant measurement $y(k)$ is taken and used to update the current estimate of the plant state using:

$$\hat{x}(k|k) = \hat{x}(k|k-1) + K(k)\left[y(k) - C(k)\hat{x}(k\ k-1)\right] \quad (3)$$

where $\hat{x}(k|k-1)$ is the state estimate at k based on measurements up to time k-1. The matrix $K(k)$ is the Kalman gain which simply weights the difference between the actual measurement $y(k)$ and the modeled estimate of $y(k)$ given by equation (2). $K(k)$ is calculated using:

$$K(k) = P(k|k-1)C^T(k)\,[C(k)P(k|k-1)C^T(k) + R(k)]^{-1} \tag{4}$$

where $R(k)$ is the covariance matrix of the measurement noise and $P(k|k-1)$ is the covariance of the error in the estimate of the state prior to the measurement. The error covariance is updated using:

$$P(k|k) = [I - K(k)C(k)]\,P(k|k-1) \tag{5}$$

Prior to taking the next measurement at time $k+1$, both the state estimate and estimate error covariance are propagated ahead in time using the state dynamics equations:

$$x(k+1|k) = \Phi(k+1,k)\hat{x}(k|k) + \Im(k)u(k) \tag{6}$$

$$P(k+1|k) = \Phi(k+1,k)P(k|k)\Phi^T(k+1,k) + Q(k) \tag{7}$$

where $Q(k)$ is the covariance matrix for the process noise vector $w(k)$. Equations (3) through (7) are processed once for each measurement.

As mentioned earlier, the GLR failure detection method uses the innovations from the Kalman filter to formulate a failure decision. The unfailed system innovations $\gamma_0(k)$ are defined as the difference between the plant measurement at $k$ and the estimate of the measurement at $k$, or using equation (2):

$$\gamma_0(k) = y(k) - C(k)\hat{x}(k|k-1) \tag{8}$$

A fundamental property of the Kalman filter, and one that is the basis for the GLR, is that for a linear system, the sequence $\gamma_0(k)$ will be white, zero-mean with covariance:

$$E[\gamma_0(k)\gamma_0^T(j)] = V(k)\delta_{k,j} \tag{9}$$

where: $V(k) = C(k)P(k|k-1)C^T(k) + R(k)$ (10)

$$\delta_{k,j} = \begin{cases} 0, & k \neq j \\ 1, & k = j \end{cases} \tag{11}$$

We now develop the procedure required to detect and identify sensor biases using the innovations described by (8)-(10).

## 2.3 Failure Decision Equations

The first step in detecting a sensor bias is to hypothesize the existence of a bias and determine its effect on the Kalman filter innovations. If a sensor bias were to occur, it would appear as an additive term in the measurement equation, i.e., a bias of magnitude $\nu$ at time $k=\theta$ would be modeled as:

$$y(k) = C(k)x(k) + v(k) + \nu\sigma_{k,\theta} \tag{12}$$

where:

$$\sigma_{k,\theta} = \begin{cases} 0, & k<\theta \\ 1, & k\geq\theta \end{cases} \tag{13}$$

Due to the linearity of the Kalman filter equations, this bias in $y(k)$ will result in a failed system innovations sequence of the form:

$$\gamma(k) = G(k,\theta)\nu + \gamma_0(k), \quad k\geq\theta \tag{14}$$

where recall $\gamma_0(k)$ is the unfailed system innovations in (8).

Equation (14) is a basic equation of the GLR. $G(k,\theta)$ is the failure signature matrix at time k assuming a sensor bias occurred at time $\theta$. To evaluate $G(k,\theta)$, we substitute equation (12) into the Kalman filter equations, compute the effect of $\nu$ on the innovations, and using (14), identify $G(k,\theta)$.

This procedure results in the recursive equations:

$$G(k,\theta) = I - C(k)\Phi(k,k-1)F(k-1,\theta) \tag{15}$$

$$F(k,\theta) = K(k)G(k,\theta) + \Phi(k,k-1)F(k-1,\theta) \tag{16}$$

$$G(k,\theta) = F(k,\theta) = 0, \quad k<\theta \tag{17}$$

Now, we have two hypotheses to examine; the no-bias hypothesis, $H_0$:

$$H_0: \quad \gamma(k) = \gamma_0(k) \tag{18}$$

and a hypothesis corresponding to a sensor bias, $H_1$:

$$H_1: \quad \gamma(k) = G(k,\theta)\nu + \gamma_0(k) \tag{19}$$

The job of the GLR is to determine which of these hypotheses is most likely to be true given the sequence of innovations, $\gamma(1)$, $\gamma(2)$, ..., $\gamma(k)$, where k is the current time. To make this decision, we assume a bias occurs at all $\theta$, $1 \leq \theta \leq k$, and for each $\theta$ value compute a maximum likelihood estimate of the bias magnitude $\hat{\nu}$. Using this estimate, we can compute the log-likelihood ratio for each $\theta$. The log-likelihood ratio, $l(k,\theta)$, is simply a measure of the probability of $H_1$ being true relative to the probability of the no bias hypothesis $H_0$ being true. The details of these computations are given in [4] and the resulting equations are:

$$\hat{\nu}(k,\theta) = J^{-1}(k,\theta)d(k,\theta) \tag{20}$$

$$l(k,\theta) = d^T(k,\theta)\hat{\nu}(k,\theta) \tag{21}$$

where $J(k,\theta)$ is the failure information matrix:

$$J(k,\theta) = \sum_{j=\theta}^{k} G^T(j,\theta)V^{-1}(j)G(j,\theta) \tag{22}$$

and $d(k,\theta)$ is the matched filter response:

$$d(k,\theta) = \sum_{j=\theta}^{k} G^T(j,\theta)V^{-1}(j)\gamma(j) \tag{23}$$

Deciding which hypothesis to accept is a relatively simple matter once each of the log-likelihood ratios has been calculated using equation (21). Since $l(k,\theta)$ is a measure of how likely it is that a sensor failure occurred at time $\theta$ given data up to time k, we choose the largest value of $l(k,\theta)$ computed and specify the corresponding value of $\theta$ to be the most likely failure time $\theta_{ML}$. We then compare this maximum log-likelihood ratio to a predetermined threshold value $\varepsilon$, and decide whether to accept hypothesis $H_0$ or hypothesis $H_1$:

$$l(k,\theta_{ML}) \underset{H_0}{\overset{H_1}{\gtrless}} \varepsilon \tag{24}$$

If we accept $H_0$, it is assumed that no failure has occurred. If we accept $H_1$ however, we assume that a sensor bias has occurred at time $\theta_{ML}$ with the bias magnitude given by equation (20):

$$\hat{v}(k,\theta_{ML}) = J^{-1}(k,\theta_{ML})d(k,\theta_{ML}) \tag{25}$$

## 3. PWR PRESSURIZER MODEL

As seen in Section 2, both the Kalman filter and failure signature matrix calculations require a plant model in the form of equations (1) and (2). In this section, we develop such a model of a PWR pressurizer. First, a nonlinear, continuous, second-order pressurizer model is derived from first principles. Then this model is linearized and discretized about a specified set of operating conditions to get the equations in the desired form.

### 3.1 Nonlinear Pressurizer Model

A typical PWR pressurizer is shown schematically in Figure 3. The pressurizer acts as a surge tank in maintaining pressure in the primary loop. In this study, the steam and water in the pressurizer are assumed to be in a homogeneous, saturated mixture. Applying mass and energy balances to this mixture using $X_p$, the mixture quality, and $P_p$, the pressurizer pressure, as state variables results in the two state equations [5]:

$$\frac{dX_p}{dt} = \frac{v_p}{V_p \Gamma} \left\{ v_p (W_{surge} + W_{spray} - W_{rv}) \left( \frac{\partial h_p}{\partial P_p} - \frac{v_p}{J} \right) + \frac{\partial v_p}{\partial P_p} \left[ Q_{htr} + W_{surge}(h_{surge} - h_p) + W_{spray}(h_{spray} - h_p) - W_{rv}(h_g - h_p) \right] \right\} \tag{26}$$

$$\frac{dP_p}{dt} = - \frac{v_p}{V_p \Gamma} \left\{ v_p \frac{\partial h_p}{\partial X_p} (W_{surge} + W_{spray} - W_{rv}) + \frac{\partial v_p}{\partial X_p} \left[ Q_{htr} + W_{surge}(h_{surge} - h_p) + W_{spray}(h_{spray} - h_p) - W_{rv}(h_g - h_p) \right] \right\} \tag{27}$$

where

$$\Gamma = \frac{\partial v_p}{\partial P_p} \frac{\partial h_p}{\partial X_p} - \frac{\partial v_p}{\partial X_p} \left( \frac{\partial h_p}{\partial P_p} - \frac{v_p}{J} \right) . \tag{28}$$

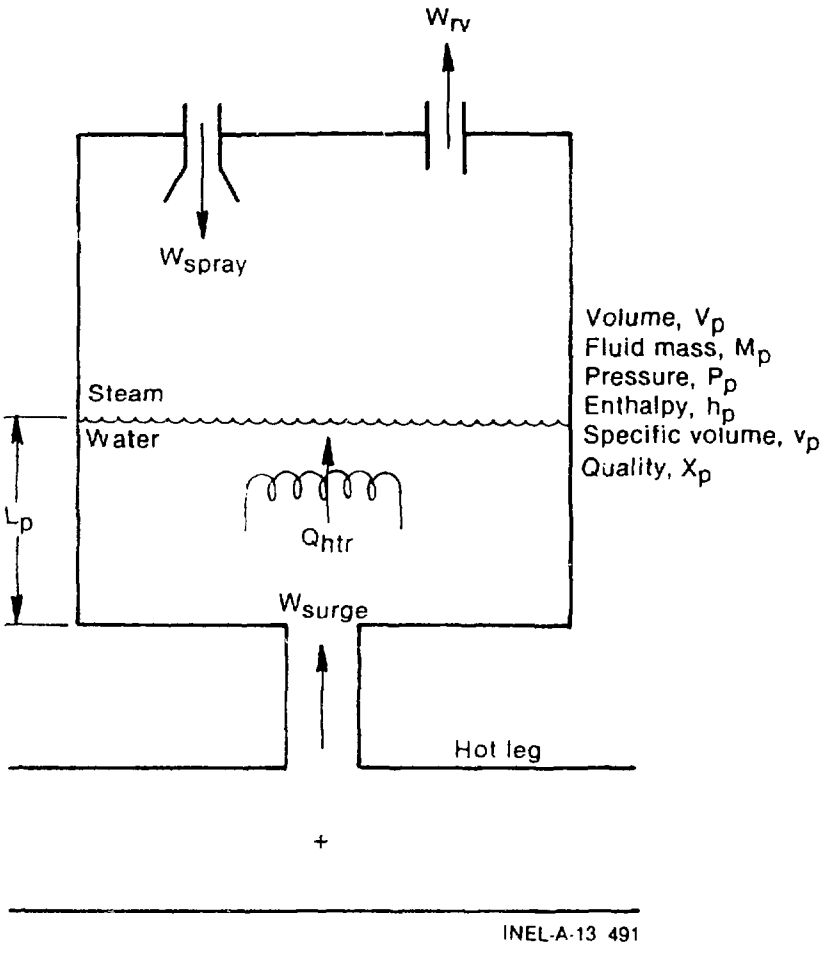


Figure 3. Pressurizer Schematic

The matrix fluid properties are defined by:

$$v_p = v_f + X_p(v_g - v_f) \tag{29}$$

$$h_p = h_f + X_p(h_g - h_f) \tag{30}$$

where $h_f$, $h_g$, $v_f$, and $v_g$ are the corresponding saturation enthalpies and specific volumes dependent on $P_p$. J is a unit conversion constant.

In (26) and (27), we note there are four inputs in the pressurizer model. The surge flow, $W_{surge}$, which is due to expansion and contraction of the primary loop fluid, is assumed to be available from plant data. The pressurizer spray, $W_{spray}$, which is tapped off from the cold leg, is used to prevent overpressurization of the primary loop. The spray is an on-off type control established by preset pressure setpoints. Similarly, the pressurizer heater output, $Q_{htr}$, and relief valve flow, $W_{rv}$, are on-off controls governed by specific setpoints.

For this model, we assume two measurements are being made, one being the water level in the pressurizer and the other being the pressurizer pressure. From (27) we see the pressure is a system state, hence the pressure measurement model is quite simple. The water level model is not quite as simple, however. The water level $L_p$ is described by:

$$L_p = A_p(1-X_p)\frac{V_p}{v_p}v_f \tag{31}$$

where $A_p$ is the cross-sectional area of the pressurizer.

## 3.2 Linear Discrete Pressurizer Model

In functional form, the nonlinear pressurizer model can be summarized as:

$$\dot{x} = f(x,u) \tag{32}$$

$$y = g(x) \tag{33}$$

where the system vectors x, u, and y are:

$$x = \begin{bmatrix} X_p \\ P_p \end{bmatrix} \tag{34}$$

$$u \quad \begin{bmatrix} W_{surge} \\ Q_{htr} \\ W_{spray} \\ W_{rv} \end{bmatrix} \tag{35}$$

$$y = \begin{bmatrix} L_p \\ P_p \end{bmatrix} \tag{36}$$

Expanding (32) and (33) about a nominal operating point $(\bar{x},\bar{u})$ in a Taylor series (ignoring terms higher than first-order) results in continuous, linear equations of the form:

$$\delta\dot{x} = A\delta x + B\delta u \tag{37}$$

$$\delta y = C\delta x \tag{38}$$

where:

$$\delta x = x - \bar{x} \tag{39}$$

$$\delta u = u - \bar{u} \tag{40}$$

$$\delta y = y - \bar{y} \tag{41}$$

Then applying standard discretization methods [6] allows (37) and (38) to be cast in the discrete form.

In order to perform simulation studies in Section 4, we need to specify a pressurizer operating point $(\bar{x},\bar{u})$ to obtain numerical values for $\Phi(k+1,k)$, $\Theta(k)$, and $C(k)$, the system matrices. In this study, we will use the geometry

of the LOFT reactor pressurizer [5] and an operating point described by:

$$\bar{x} = \begin{bmatrix} 0.09591 \\ 2145.1 \end{bmatrix} \begin{matrix} (-) \\ (\text{psia}) \end{matrix} \tag{42}$$

$$\bar{u} = \begin{bmatrix} 0.0 \\ 0.0 \\ 0.0 \\ 0.0 \end{bmatrix} \begin{matrix} (\text{lbm/s}) \\ (\text{Btu/s}) \\ (\text{lbm/s}) \\ (\text{lbm/s}) \end{matrix} \tag{43}$$

$$\bar{y} = \begin{bmatrix} 41.73 \\ 2145.1 \end{bmatrix} \begin{matrix} (\text{in}) \\ (\text{psia}) \end{matrix} \tag{44}$$

Using these values, applying the above described techniques, and adding in process and measurement noise yields the linear, discrete pressurizer model in the form of (1) and (2):

$$\begin{bmatrix} X_p(k+1)-0.09591 \\ P_p(k+1)-2145.1 \end{bmatrix} = \begin{bmatrix} 1 & 0 \\ 0 & 1 \end{bmatrix} \begin{bmatrix} X_p(k)-0.09591 \\ P_p(k)-2145.1 \end{bmatrix} \tag{45}$$

$$+ \begin{bmatrix} -2.898\text{E-}4 & 4.303\text{E-}7 & -3.548\text{E-}4 & 1.019\text{E-}4 \\ 8.102\text{E-}1 & 1.007\text{E-}2 & -7.102\text{E-}1 & -5.208\text{E0} \end{bmatrix} \begin{bmatrix} W_{surge}(k) \\ Q_{htr}(k) \\ W_{spray}(k) \\ W_{pv}(k) \end{bmatrix} + w(k)$$

$$\begin{bmatrix} L_p(k)-41.73 \\ P_p(k)-2145.1 \end{bmatrix} = \begin{bmatrix} -195.2 & 337.3 \\ 0 & 1 \end{bmatrix} \begin{bmatrix} X_p(k)-0.09591 \\ P_p(k)-2145.1 \end{bmatrix} + v(k) \tag{46}$$

## 4. SIMULATION RESULTS

To demonstrate the capabilities of the GLR technique in identifying pressurizer sensor biases, several simulation studies were performed. The results of one such study are presented here.

Simulated pressurizer level and pressure measurements during a typical PWR transient were obtained using the nonlinear pressurizer model described in Section 3.1. The model was initialized at the steady state operating point defined in (42), i.e.:

$$x = \begin{bmatrix} x_p \\ P_p \end{bmatrix} = \begin{bmatrix} 0.09591 \\ 2145.1 \end{bmatrix} \tag{42}$$

and then perturbed by fluctuations in the surge flow. The calculated level and pressure measurements, which include some measurement noise, were then used in the Kalman filter equations of the GLR scheme. The Kalman filter and GLR bias detection equations were based on the linear, discrete pressurizer model given by (45) and (46). Assumed process and measurement noise covariance matrices were:

$$Q(k) = \begin{bmatrix} 2.30E\text{-}9 & 0 \\ 0 & 1.15 \end{bmatrix} \tag{47}$$

$$R(k) = \begin{bmatrix} 0.01 & 0 \\ 0 & 4.0 \end{bmatrix} \tag{48}$$

Figures 4 and 5 display the plant measurements as calculated using the nonlinear pressurizer model and the measurements as estimated by the Kalman filter. In this study, a +0.5 inch bias was added into the pressurizer level measurement at t=50 seconds to see if the GLR technique could identify the existence of such a bias. Examining Figure 4, we see the filter estimate

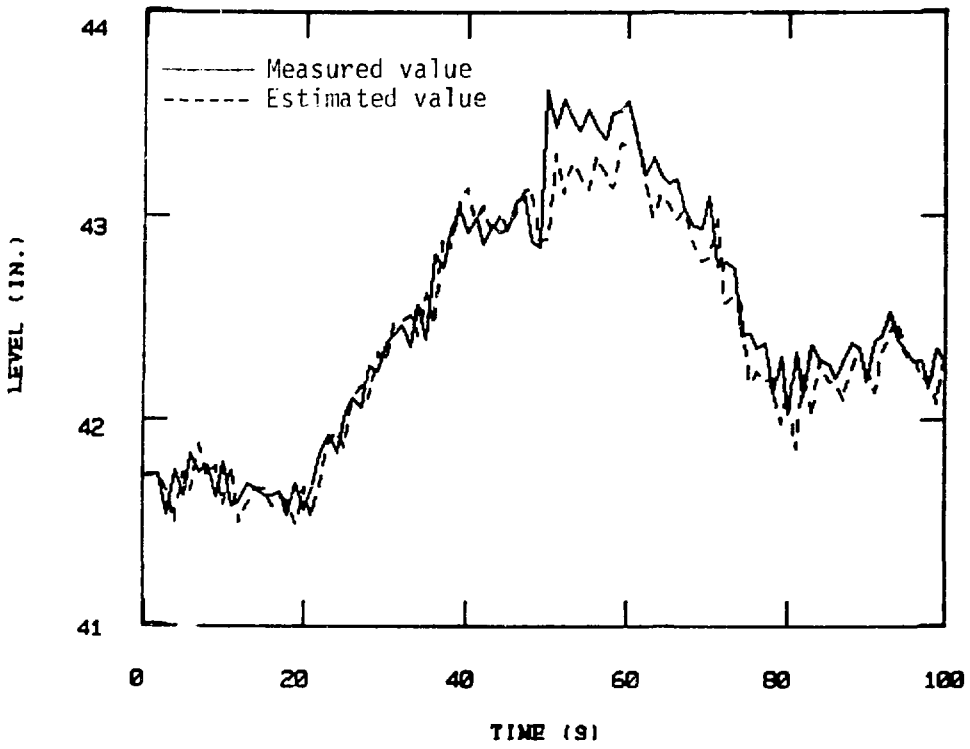


Figure 4. Typical Plant Transient, Comparison of Measured and Estimated Pressurizer Level

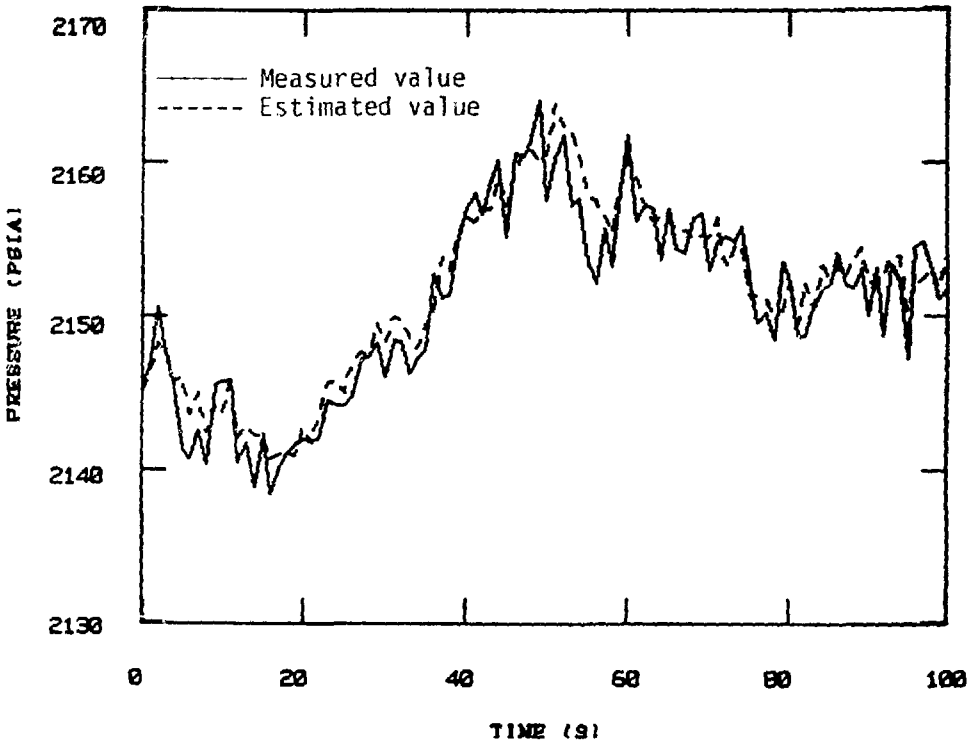


Figure 5. Typical Plant Transient, Comparison of Measured and Estimated Pressurizer Pressure

of water level follows the plant measurement quite well prior to the implementation of the bias at 50 seconds. After 50 seconds, the measurement bias is seen to cause a corresponding bias in the Kalman filter estimate. Similar effects are noted in the pressurizer pressure traces in Figure 5.

The maximum log-likelihood ratio, $l(k,\theta)$, computed using the GLR equations during this plant transient is shown in Figure 6. Prior to the bias at 50 seconds, the ratio stays relatively small. Following the bias implementation, however, the maximum value of $l(k,\theta)$ increases dramatically indicating a failure, or sensor bias, has probably occurred. The time that such a bias would be detected, and hence the estimated bias value and failure time, would of course depend on the threshold value $\varepsilon$ applied to the curve in Figure 6. As an example, using $\varepsilon$=75 on this curve resulted in the bias being detected at k=53 seconds. The failure time $\theta$, was estimated to be 50 seconds, and the failure or bias magnitude estimate was $\nu$=0.54 inches. Hence, the GLR scheme provided nearly exact bias identification in this case. Different $\varepsilon$ values will yield different results. In practice, the choice of what $\varepsilon$ to use would be made by considering tradeoffs between false alarm probabilities and bias detection probabilities.

A final point to note in Figure 6 is that the maximum log-likelihood ratio begins to decrease about 10 seconds after the bias implementation. Recall from Section 2, the GLR requires that for each k, a value of $l(k,\theta)$ is computed for all $\theta$, $1 \leq \theta \leq k$. This requires a growing bank of matched filters and hence an ever-increasing amount of data storage. To eliminate this problem, what is typically done is to restrict candidate $\theta$ values to a sliding data window of the form:

$$k-N \leq \theta \leq k-M \tag{49}$$

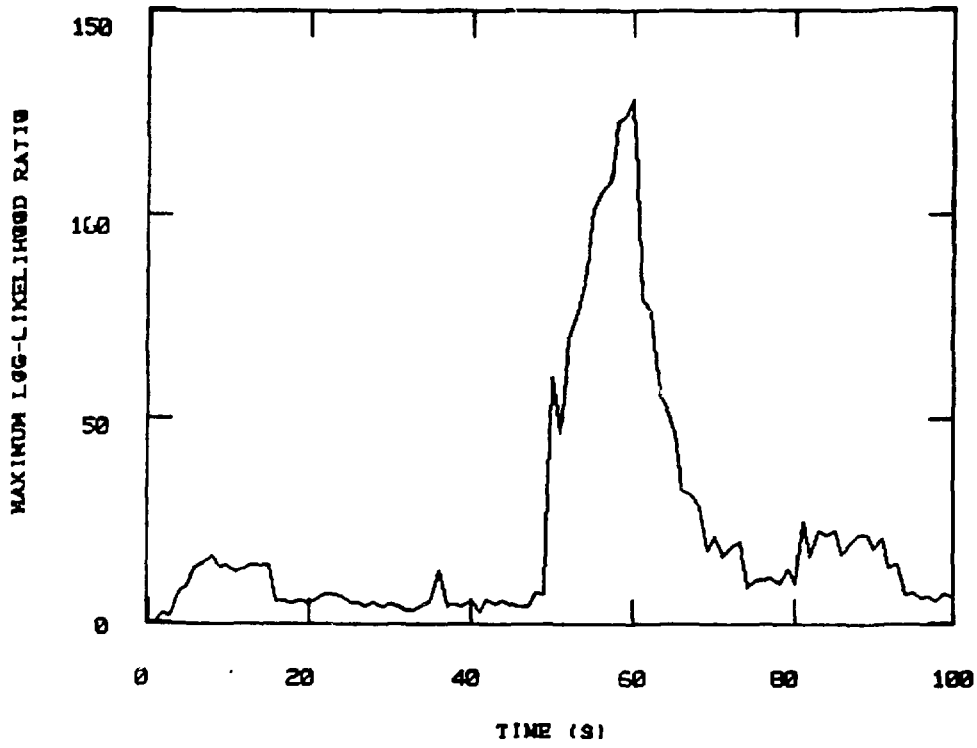


Figure 6. Maximum Log-Likelihood Ratio

This simplification does not lead to serious difficulties as long as the window length, N-M, is large enough to insure detection and identification of all significant sensor biases. Such a window was implemented in calculating the values of $l(k,\theta)$ shown in Figure 6; values of M=0 and N=10 were used in the window. This windowing has the effect of implementing the GLR technique as a finite memory filter [2]. So once the failure time is no longer in the data window, i.e., $\theta<k-10$, $l(k,\theta)$ will decrease, and the detection law will become less likely to select $H_1$, the failure hypothesis.

## 5. CONCLUSIONS

With the recent incidents at Three Mile Island and other nuclear facilities, there is a renewed interest in the protection and control of nuclear power plants. Specifically, much attention is being paid to the problem of supplying the plant operator with the information needed to properly ascertain the plant status. The generalized likelihood ratio failure detection method described in this paper could be a powerful tool in achieving that goal. We have shown here that the GLR is capable of detecting biases in PWR pressurizer instruments. Using straightforward extensions to the GLR scheme, we could also have the capability of detecting complete sensor failures, failures of actuators such as the pressurizer relief valves and heaters, or detecting inherent changes in the plant dynamics and distinguishing between such dynamics changes and sensor failures. Furthermore, implementing the GLR using a complete PWR plant model such as that described in [5] would allow the development of a total plant failure monitor. Before proceeding with such expansions, however, some further work must be done using the existing pressurizer instrumentation bias identification scheme.

An obvious requirement for practical application of the GLR at a nuclear facility is that it have the capability of real-time operation. To test this capability, the bias detection scheme will be implemented on a PDP 11/55 minicomputer and connected to a real-time hybrid computer model of the LOFT reactor plant. Using this model to provide simulated plant transient data, the real-time performance of the GLR will be investigated.

To make the linear, discrete model of the pressurizer inherent in the GLR more representative of the actual LOFT pressurizer, several modifications must be made. In the actual pressurizer, three level measurements are made; the linear model should be augmented to reflect this redundancy. A measurement not used in this study, that being the temperature of the vapor space in the pressurizer, should also be modeled. Also, it may be necessary to use a higher-order dynamic model, perhaps using individual mass and energy balances on both fluid regions, in order to be more representative of the actual pressurizer dynamics.

Following these model modifications and the hybrid computer simulation studies, a final test of the GLR failure monitor would be to install the PDP minicomputer (which would have all the necessary GLR software) at the LOFT facility. Using the GLR techniques during actual LOFT operation would perhaps demonstrate the feasibility of commercial implementation.

## 6. ACKNOWLEDGMENT

Work supported by the U.S. Nuclear Regulatory Commission, Office of Reactor Safety Research under DOE Contract No. DE-AC07-76ID01570.

## 7. REFERENCES


1. Willsky, A. S., "A Survey of Design Methods in Failure Detection in Dynamic Systems," Automatica, Volume 12, Pergamon Press, 1976.
2. Willsky, A. S. and Jones, H. L., "A Generalized Likelihood Ratio Approach to the Detection and Estimation of Jumps in Linear Systems," IEEE Transactions on Automatic Control, February 1976.
3. Sage, A. P. and Melsa, J. L., Estimation Theory with Applications to Communications and Control, Robert E. Krieger Publishing Company, Huntington, New York, 1979.
4. Melsa, J. L. and Cohn, D. L., Decision and Estimation Theory, McGraw-Hill Book Company, New York, 1978.
5. Tylee, J. L., "Low-Order Model of the LOFT Reactor Plant for Use in Kalman Filter-Based Optimal Estimators," EGG-2006, January 1980.
6. Kuo, B. C., Digital Control Systems, SRL Publishing Company, Champaign, Illinois, 1977.